

Simulation of bedform formation using an Eulerian two-phase flow model.

A. Mathieu *CACR, University of Delaware, Newark, DE, USA – amathieu@udel.edu*

A. Salimi-Tarazouj *NWS/NCEP/EMC, NOAA, University of Maryland, College Park MD, USA*

T.-J. Hsu *CACR, University of Delaware, Newark, DE, USA*

C. Bonamy *LEGI, University of Grenoble Alpes, G-INP, CNRS, 38000 Grenoble, France*

J. Chauchat *LEGI, University of Grenoble Alpes, G-INP, CNRS, 38000 Grenoble, France*

ABSTRACT: A full understanding of the mechanisms responsible for bedform formation is not yet achieved. In this work, we apply a new tool, an Eulerian turbulence-resolving two-phase model, to investigate the formation of ripples starting from an initially flat bed. An experimental configuration is reproduced numerically and numerical experiments are performed to assess the predictive capabilities of the two-phase model. Although the results show a grid-size dependency, the main features of ripple formation are reproduced by the model. Results show the important role played by turbulent coherent structures in the early stage of ripple formation. We hypothesize that the grid-size dependency is related to timescale of ripple evolution and closure models.

1 INTRODUCTION

The evolution of bedforms in the fluvial and coastal environment has been investigated for more than a century (Bucher 1919, Engelund & Fredsoe 1982, Best 2005, Charru et al. 2013). Yet, no consensus on the mechanisms responsible for the generation of bedforms has been reached. Significant insight on the initiation of bedforms has been revealed by both linear stability analysis and experimental observations (Kennedy 1963, Kuru et al. 1995, Fourrière et al. 2010, Perillo et al. 2014). However, from the numerical point of view, the large spectrum of spatial and temporal scales involved in bedform formation makes simulation of the phenomenon extremely challenging, especially for the investigation of the role played by small scale turbulent coherent structures on the subsequent morphological evolution into larger benthometric features. Recent developments in turbulence-resolving

Eulerian two-phase flow modelling represent a good opportunity to tackle this challenge (Mathieu et al. 2021, Mathieu et al. 2022). In the Eulerian two-phase flow model, both the carrier and the dispersed phase composed of sediment particles are seen as a continuum. Using the Eulerian two-phase flow model is a good compromise between computationally expensive Lagrangian two-phase flow methodologies for which individual particle dynamics have to be computed and single phase flow models for which sediment transport is assumed as empirical bedload and suspended load and bed morphology relies on the Exner equation.

In this study, we apply for the first time the turbulence-resolving Eulerian two-phase flow methodology to investigate bedform formation from a flat bed in a unidirectional flow. The model and numerical configurations are presented in section 2, results are shown and discussed in section 3, then, conclusions are drawn in section 4.

2 MATERIAL AND METHODS

2.1 Eulerian two-phase flow model

The turbulence-resolving two-phase model sedFoam (Chauchat et al. 2017, Mathieu et al. 2021) (<https://github.com/SedFoam/sedfoam>) is used to simulate the formation of bedforms in unidirectional flows using the Large-Eddy Simulation (LES) methodology.

2.1.1 Governing equations

In the Eulerian two-phase flow formalism, coupled mass and momentum conservation equations for the fluid and the solid phases are solved. The mass conservation for the fluid and the solid phase are given by

$$\frac{\partial(1-\phi)}{\partial t} + \frac{\partial(1-\phi)u_i^f}{\partial x_i} = 0 \quad (1)$$

$$\frac{\partial\phi}{\partial t} + \frac{\partial\phi u_i^s}{\partial x_i} = 0 \quad (2)$$

respectively with \mathbf{x} the position vector, $i=1,2,3$ representing the streamwise, vertical and spanwise components, ϕ the filtered sediment concentration and u_i^f , and u_i^s the fluid and solid Favre filtered velocities.

The fluid and solid momentum conservation equation are written as

$$\begin{aligned} \frac{\partial\rho^f(1-\phi)u_i^f}{\partial t} + \frac{\partial\rho^f(1-\phi)u_i^f u_j^f}{\partial x_j} = \\ -(1-\phi)\frac{\partial P^f}{\partial x_i} + \frac{\partial}{\partial x_i} [T_{ij}^f + \sigma_{ij}^f] \\ -I_i + \rho^f(1-\phi)g_i + (1-\phi)f_i^v \end{aligned} \quad (3)$$

$$\begin{aligned} \frac{\partial\rho^s\phi u_i^f}{\partial t} + \frac{\partial\rho^s\phi u_i^s u_j^s}{\partial x_j} = -\phi\frac{\partial P^f}{\partial x_i} - \frac{\partial P^s}{\partial x_i} \\ + \frac{\partial}{\partial x_i} [T_{ij}^s + \sigma_{ij}^s] + I_i + \rho^s\phi g_i + \phi f_i^v \end{aligned} \quad (4)$$

With ρ^f and ρ^s the fluid and solid densities and P^f and P^s the fluid and solid phase pressures. The effective fluid and solid stress tensors T^f and T^s are given by

$$T_{ij}^f = \rho^f(1-\phi)v^f \left(\frac{\partial u_j^f}{\partial x_i} + \frac{\partial u_i^f}{\partial x_j} - \frac{2}{3} \frac{\partial u_k^f}{\partial x_k} \delta_{ij} \right) \quad (5)$$

$$T_{ij}^s = \rho^s\phi v^s \left(\frac{\partial u_j^s}{\partial x_i} + \frac{\partial u_i^s}{\partial x_j} - \frac{2}{3} \frac{\partial u_k^s}{\partial x_k} \delta_{ij} \right) \quad (6)$$

Where v^f and v^s are the fluid and solid phases viscosities, g_i is the acceleration of gravity and f^v a volume force driving the flow. Coming from the filtering of the non-linear advection term, σ^f and σ^s are the sub-grid scale stress tensors. The momentum exchange term between the two phases I is modelled using a drag law.

Table 1: Flow, particle and numerical parameters

Configurations	$h(m)$	$u_\tau(m/s)$	$d_p(mm)$	Re_τ	L_x/h	L_z/h	Δx^+	Δz^+	Δy^+ (interface)
Venditti - coarse	0.150	0.028	0.5	4,200	6.3	3.1	114	57	20.0
Venditti - fine	0.150	0.028	0.5	4,200	6.3	3.1	75	38	14.0
Num. Exp. 1 - coarse	0.075	0.020	0.5	1,500	6.3	3.1	25	13	3.0
Num. Exp. 2 - coarse	0.050	0.020	0.5	1000	9.4	4.7	25	13	3.0
Num. Exp. 3 - coarse	0.025	0.020	0.5	500	18.8	9.4	25	13	3.0
Num. Exp. 3 - fine	0.025	0.020	0.5	500	18.8	9.4	20	9	2.4

2.1.2 Closure models

In the LES framework, the effect of the unresolved turbulent scales are taken into account by modelling the sub-grid scale stress tensors. In our study, σ^f and σ^s are modelled using the dynamic Lagrangian methodology derived for the two-phase model by Mathieu et al. (2021).

To represent to complex behaviour of the dispersed solid phase, the solid phase pressure and viscosities are modelled using the kinetic theory for granular flows from Chassagne et al. (submitted) coupled with a frictional model at high volume fraction (Johnson & Jackson 1997, Schaeffer 1987).

2.2 Numerical set-up

In this study, we present six different configurations to assess the predictive capabilities of the two-phase flow model. Two configurations reproduce the experimental configuration from Venditti et al. (2005) designed to investigate the mechanisms of bedform formation. This configuration consists of an unidirectional flow having a depth $h=0.15\text{m}$ developing over a flat sediment bed composed of particles having a median diameter $d_p=0.5\text{mm}$. The Reynolds number Re_τ based on the friction velocity $u_\tau=0.028\text{m}\cdot\text{s}^{-1}$ is equal to 4,200. The two configurations investigated differ by the numerical resolution in order to investigate the grid size dependency. Information on the grid size in wall units for all the configurations are presented in Table 1 together with flow and particle parameters.

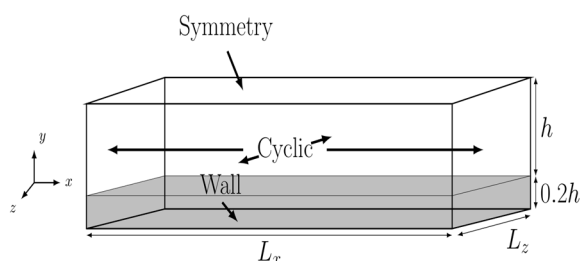


Figure 1: Sketch of the numerical domain and boundary conditions

Four other configurations are performed as numerical experiments for which there is no experimental data for comparison to investigate the effect of the water depth and grid resolution on the bedform development. Compared with the experimental configuration of Venditti et al. (2005), these numerical experiments have a smaller water depth ($h=0.075, 0.05$ and 0.025m) and a lower friction velocity $u_\tau=0.02\text{m}\cdot\text{s}^{-1}$ resulting in a lower Reynolds number $Re_\tau=1500, 1000$ and 500 . Consequently, we can significantly increase mesh resolution and better resolve the interactions between the fluid turbulence and the sediment bed.

The numerical domain for all six configurations consists of a periodic box with cyclic boundary conditions in the streamwise and spanwise directions, a symmetry plane at the top and a deposited sediment bed having a depth $0.2 h$ at the bottom (see Figure 1). It differs between the configurations in the water depth, the mesh resolution and dimensions in the streamwise and spanwise directions (L_x and L_z respectively).

3 RESULTS

For all the configurations presented in this study, bedforms develop spontaneously at the top of the sediment bed everywhere in the numerical domain consistently with the observations of Venditti et al. (2005).

Table 2: Quasi-2D ripple length predicted by the two-phase model compared with experimental results

Configurations	$\lambda_{2D}(\text{Num})$	$\lambda_{2D}(\text{Exp})$
<u>Venditti</u> - coarse	0.103 m	0.110 m
<u>Venditti</u> - fine	0.059 m	0.110 m
Num. Exp. 1 - coarse	0.028 m	-
Num. Exp. 2 - coarse	0.029 m	-
Num. Exp. 3 - coarse	0.030 m	-
Num. Exp. 3 - fine	0.026 m	-

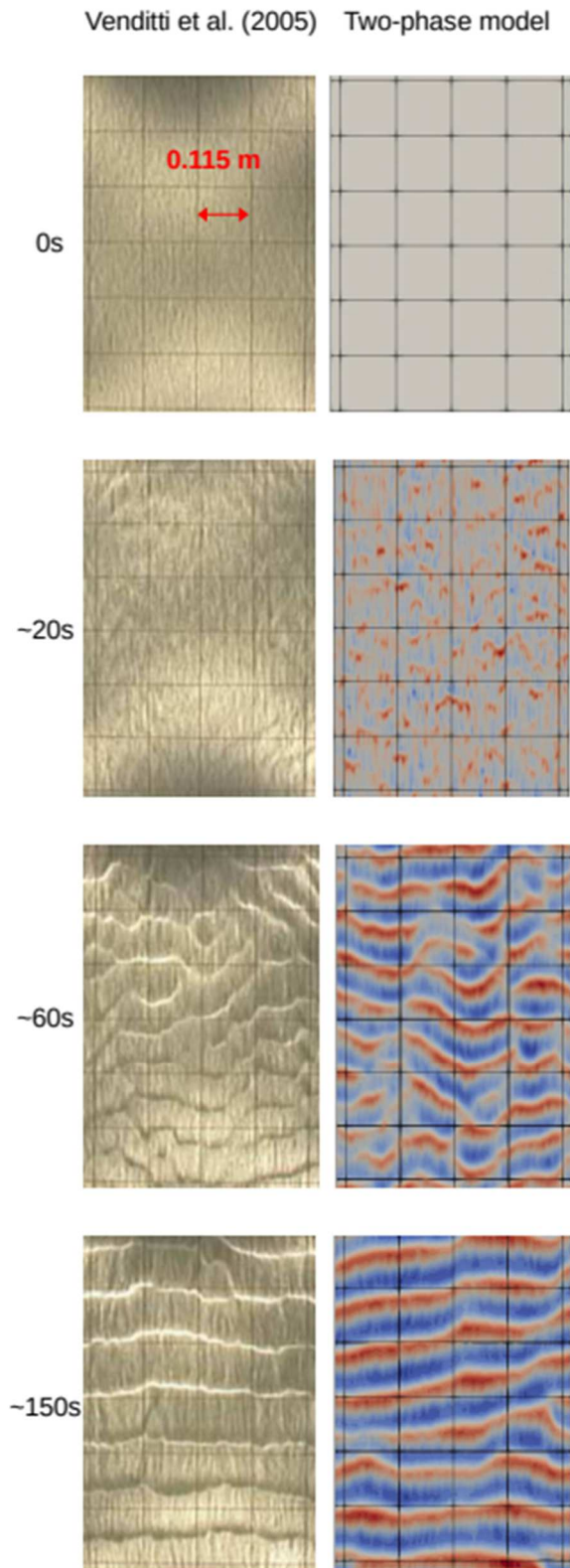


Figure 2: Snapshots of the bed from experimental configuration of Venditti et al. (2005) (left) and numerical simulation with coarse mesh (right) at different times.

Highly unstable in the first few seconds, initial bed defects taking the form of streamwise sediment ridges generated by turbulent coherent structures rapidly transition to more stable quasi 2D ripples having an identifiable length-scale λ_{2D} . This length-scale is presented in Table 2 for all the configurations.

It appears that for the two configurations aiming at reproducing the experiment from Venditti et al. (2005), there is a difference in the length-scale λ_{2D} predicted by the two-phase model for a different resolution. Using a coarser mesh gives a larger λ_{2D} ripple length closer to measured data.

Snapshots of the bed taken from the experimental configuration of Venditti et al. (2005) and the numerical simulation using the coarser mesh are presented in Figure 2. The comparison between experiments and the simulation show that the spatio-temporal development of bedforms is qualitatively reproduced by the two-phase model. Starting from a flat bed, turbulent coherent structures drives the generation of small flow parallel sediment ridges which then rapidly evolve into cross-hatch pattern which eventually transition to quasi 2D ripples.

The qualitative prediction of the temporal evolution of bedform formation shows that the turbulence-resolving Eulerian two-phase flow model can potentially be a great tool to investigate the role of the flow hydrodynamics and the fluid turbulence on the mechanisms driving in the initial stage of bedform development. However, it seems that simulation results are significantly affected by the mesh resolution. Grid size dependency needs to be investigated before the model can be used to predict ripple evolution, which is known to strongly depend on grain size and flow intensity.

For the numerical experiments, the predicted λ_{2D} slightly increases for decreasing water depth. However, this increase can not be considered significant considering that λ_{2D} only increases by 7% for a water depth smaller by a factor 3. This confirms that our numerical experiments lie in the ripple regime for which the length-

scale associated with the bedform is independent of the water depth.

Snapshots of the bed elevation for the three numerical experiments using a coarse resolution are shown on Figure 3.

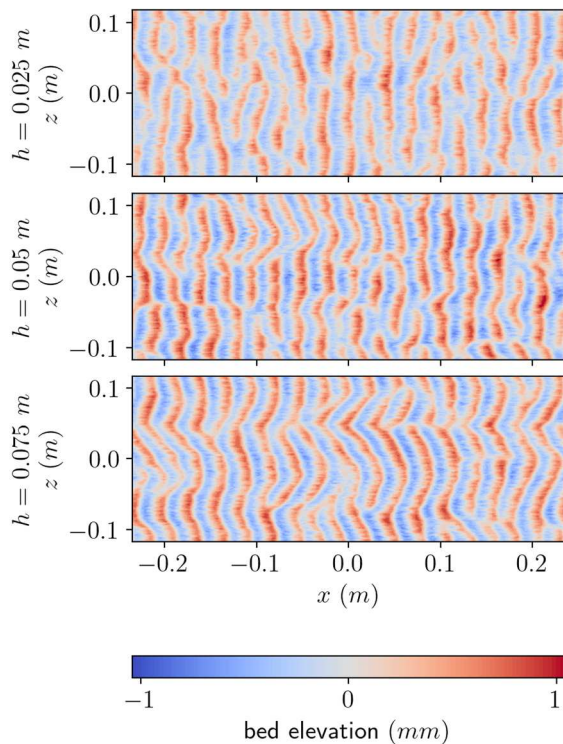


Figure 3: Colormaps of bed elevation for numerical experiments 1, 2 and 3 using the coarser mesh at the quasi-2D stage of ripple development

Even if the streamwise length-scale associated with the ripples is similar for the three numerical experiments, it appears from Figure 3 that the spanwise morphological evolution of the bed is more affected by the water depth with more sinuous ripples for increasing water depth. This can be attributed to the interaction between the ripples and the large-scale turbulent structures scaling with the water depth.

Similarly to the configurations reproducing the experimental configuration of Venditti et al. (2005), the ripple length predicted for the numerical experiment 3 is sensitive to the mesh resolution.

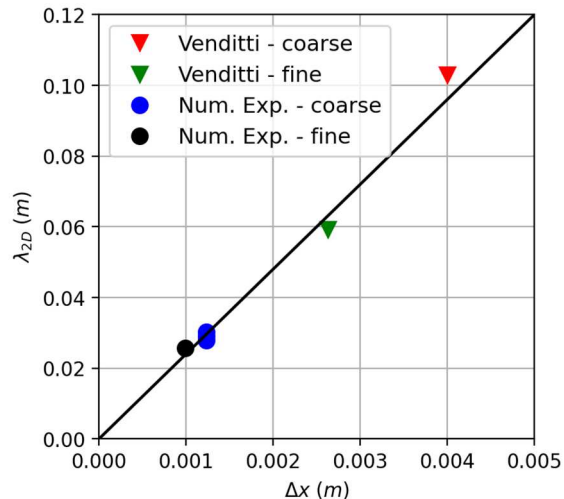


Figure 4: Predicted ripple length by the Eulerian two-phase flow model as a function of the grid size in the streamwise direction

Figure 4 confirms that there is a clear dependency between the predicted ripple length and the grid size in the streamwise direction. This issue needs to be addressed in the future by more comprehensive grid convergence test and comparison with linear stability analysis to determine its origin and to be able to quantitatively predict the spatio-temporal evolution of the ripple formation process.

4 CONCLUSIONS

In this study, numerical simulations of bedform formation in an unidirectional flow starting from a flat bed using a turbulence-resolving Eulerian two-phase flow model are presented. It is the first attempt to apply this modelling methodology to bedform formation configurations. Using turbulence-resolving two-phase flow model can significantly improve our understanding of the mechanisms at the origin of bedform formation, especially the interactions between the turbulent coherent structures and the sediment bed.

Two configurations reproducing an experiment if Venditti et al. (2005) and four additional numerical experiments allowed to investigate the effect of the water depth and the numerical resolution on the predicted ripple length. Comparison between snapshots of the resolved bathymetry from the

experiment and the simulation showed that the main features of the spatio-temporal evolution of bedform are reproduced by the two-phase model. The numerical experiments showed that the dependency between the predicted quasi-2D ripple length and the water depth is not significant as should be expected in the ripple regime. However, numerical results show a grid-size dependency. This issue needs to be addressed in the future.

5 REFERENCES

- Best, J., 2005. The fluid dynamics of river dunes: A review and some future research directions. *Journal of Geophysical Research – Earth Surface*, 110, F04S02, doi:10.1029/2004JF000218
- Bucher, W.H., 1919. On ripples and related sedimentary surface forms and their paleogeographic interpretation. *American Journal of Science*, s4-47 (279), 149-210, doi:10.2475/ajs.s4-47.279.149
- Charru, F., Andreotti, B., Claudin, P., 2013. Sand Ripples and Dunes. *Annual Review of Fluid Mechanics*, 45, 469-493, doi:10.1146/annurev-fluid-011212-140806
- Chassagne, R., Chauchat, J., Bonamy, C., (submitted). *Journal of Fluid Mechanics*
- Chauchat, J., Cheng, Z., Nagel, T., Bonamy, C., Hsu, T.-J., 2017. SedFoam-2.0: a 3-D two-phase flow numerical model for sediment transport. *Geoscientific Model Development*, 10, 4367-4392, doi:10.5194/gmd-10-4367-2017
- Engelund, F., Fredsoe, J., 1982. Sediment Ripples and Dunes. *Annual Review of Fluid Mechanics*, 14, 13-37, doi:10.1146/annurev.fl.14.010182.000305
- Fourrière, A., Claudin, P., Andreotti, B., 2010. Bedforms in a turbulent stream: formation of ripples by primary linear instability and of dunes by nonlinear pattern coarsening. *Journal of Fluid Mechanics*, 649, 287-328, doi:10.1017/S0022112009993466
- Johnson, P.C., Jackson, R., 1987. Frictional-collisional constitutive relations for granular materials, with application to plane shearing. *Journal of Fluid Mechanics*, 176, 67-93. doi:10.1017/S0022112087000570
- Kennedy, J.F., 1963. The mechanics of dunes and antidunes in erodible-bed channels. *Journal of Fluid Mechanics*, 16(4), 521-544. doi:10.1017/S0022112063000975
- Kuru, W.C., Leighton, D.T., McCready, M.J., 1995. Formation of waves on a horizontal erodible bed of particles. *International Journal of Multiphase Flow*, 6, 1123-1140, doi:10.1016/0301-9322(95)00035-V
- Mathieu, A., Chauchat, J., Bonamy, C., Balarac, G., Hsu, T.-J. (2021). A finite-size correction model for two-fluid large-eddy simulation of particle-laden boundary layer flow. *Journal of Fluid Mechanics*, 913, A26. doi:10.1017/jfm.2021.4
- Mathieu, A., Cheng, Z., Chauchat, J., Bonamy, C., Hsu, T.-J. (2022). Numerical investigation of unsteady effects in oscillatory sheet flows. *Journal of Fluid Mechanics*, 943, A7. doi:10.1017/jfm.2022.405
- Perillo, M., Best, J., Yokokawa, M., Sekiguchi, T., Takagawa, T., Garcia, M., 2014. A unified model for bedform development and equilibrium under unidirectional, oscillatory and combined-flows. *Sedimentology*, 61(7), 2063-2085, doi:10.1111/sed.12129
- Schaeffer, D., 1987. Instability in the evolution equations describing incompressible granular flow. *Journal of Differential Equations*, 66(1), 19-50, doi:10.1016/0022-0396(87)90038-6
- Venditti, J., Church, M., Bennett, S., 2005. Bed form initiation from a flat sand bed. *Journal of Geophysical Research – Earth Surface*, 110, F01009, doi:10.1029/2004JF000149.